Supporting Information

Pseudorotaxane capped mesoporous silica nanoparticles for 3,4-methylenedioxymethamphetamine (MDMA) detection in water

General techniques: Powder X-ray diffraction (PXRD), thermogravimetric analysis (TGA), elemental analysis, transmission electron microscopy (TEM), N_2 adsorption-desorption, UV-visible (UV-vis) and fluorescence spectroscopy were employed to characterize synthesized materials. PXRD measurements were taken on a D8 Advance diffractometer using CuKα radiation (Philips, Amsterdam, The Netherlands). Thermogravimetric analyses were carried out on a TGA/SDTA 851e balance (Mettler Toledo, Columbus, OH, USA) in an oxidizing atmosphere (air, 80 mL min^{-1}) with a heating program: gradient of 393-1273 K at 10°C min^{-1}, followed by an isothermal heating step at 1273°C for 30 min. TEM images were obtained with a 100 kV CM10 microscope (Philips). N_2 adsorption-desorption isotherms were recorded with a Tristar II Plus automated analyzer (Micromeritics, Norcross, GA, USA). The samples were degassed at 120°C in vacuum overnight. Specific surface areas were calculated from the adsorption data within the low pressure range using the Brunauer, Emmett and Teller (BET) model. Pore size was determined following the Barret, Joyner and Halenda (BJH) method. Fluorescence spectroscopy measurements were taken on a Felix 32 Analysis, version 1.2 (Build 56, Photon Technology International, Birmingham, NJ, USA), and by a JASCO FP-8500 spectrophotometer.

Chemicals: Tetraethylorthosilicate (TEOS), *n*-cetyltrimethylammonium bromide (CTAB), sodium hydroxide, (3-isocyanatopropyl)triethoxysilane, 1-naphtol, 2-bromoethanol, triethylamine, fluorescein,

MDMA, acetonitrile, methanol and TFH were purchased from Sigma-Aldrich Química (Madrid, Spain). All the products were used as received. Other drugs tested, morphine, methadone, heroin and cocaine were kindly provide by "Agencia Española de Medicamentos y Productos Sanitarios" (AEMPS).

Synthesis of MCM-41 mesoporous nanoparticles: NaOH (2.00 mol L^{-1}, 3.5 mL) was added to a solution of CTAB (1.00 g, 2.74 mmol) in deionized H_2O (480 mL). The solution temperature was adjusted to 80°C and then TEOS (5.00 mL, 2.57×10^{-2} mol) was added dropwise to the surfactant mixture. The mixture was stirred for 2 h to give a white precipitate. The solid was isolated by centrifugation and washed with deionized H_2O and EtOH, and then dried at 60°C for 12 h to give MCM-41. In order to remove the template phase, MCM-41 was calcined at 550°C in an oxidizing atmosphere.

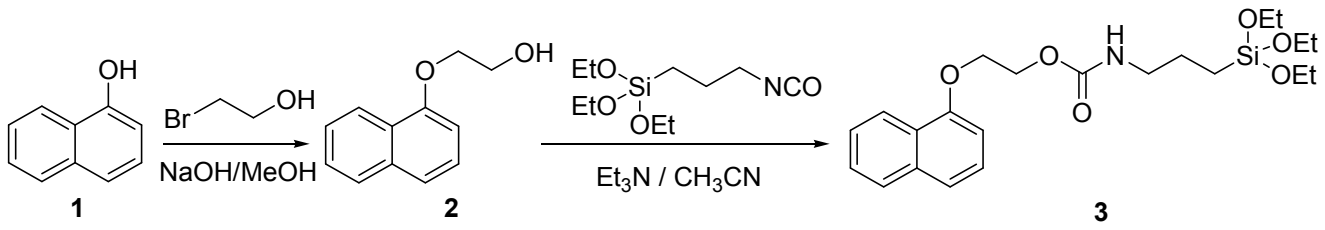

Scheme S1. Synthetic procedure used for the preparation of naphtol derivative **3**.

Synthesis of 2-(1-Naphthyloxy) ethanol (2): 1-naftol (**1**; 1 g, 6.93 mmol) was dissolved in MeOH (20 mL) and then NaOH (0.30 g, 7.63mmol) was added to the solution. The mixture was maintained at room temperature for 1 h and then the solvent was removed under reduced pressure. In a second step, the sodium salt was re-dissolved in anhydrous THF and then 2-bromoethanol was added dropwise. The reaction was stirred overnight at room temperature under Argon atmosphere. The crude product was purified in silica column with hexane-ethyl acetate 60:40, as eluent (0.12 g, 4.85 mmol, yield 70%). ^{1}H NMR (400 MHz, $CDCl_3$) δ 7.75 (m, 3H), 7.45 (t, J=8.0Hz, 1H), 7.35 (t, J=7.2, Hz 1H), 7.17 (m, 2H), 4.22 (t, J=4.8 Hz, 2H), 4.03 (c, J=4.0 Hz, 2H) ppm. ^{13}C NMR (101 MHz, $CDCl_3$) δ 156.53, 134.48, 129.55, 129.15, 127.67, 126.78, 126.47, 123.87, 118.71, 106.89, 69.21, 61.52 ppm. HRMS-EI *m/z*: calcd for $C_{12}H_{12}O_2$+H^+: 189.0905; measured: 189.0911.

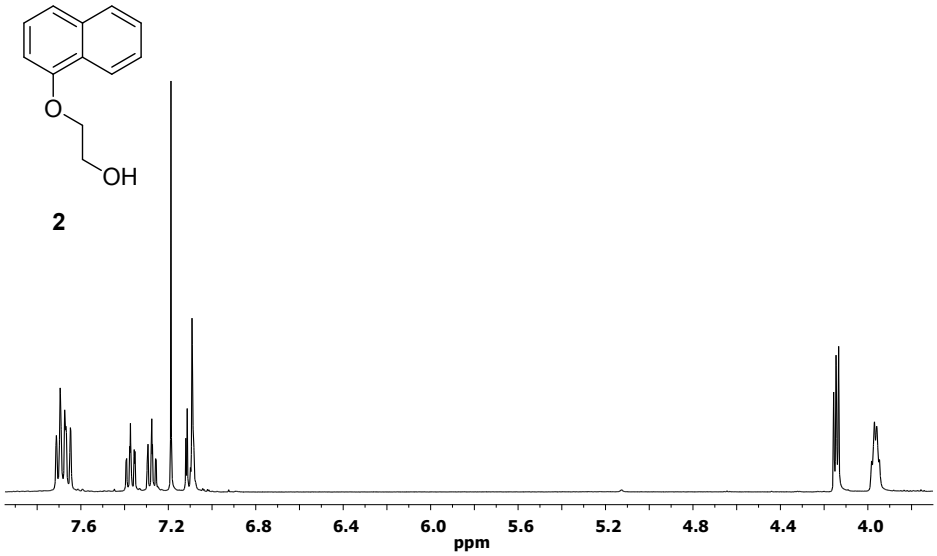

Figure S1. ^{1}H NMR spectrum of **2** in $CDCl_3$.

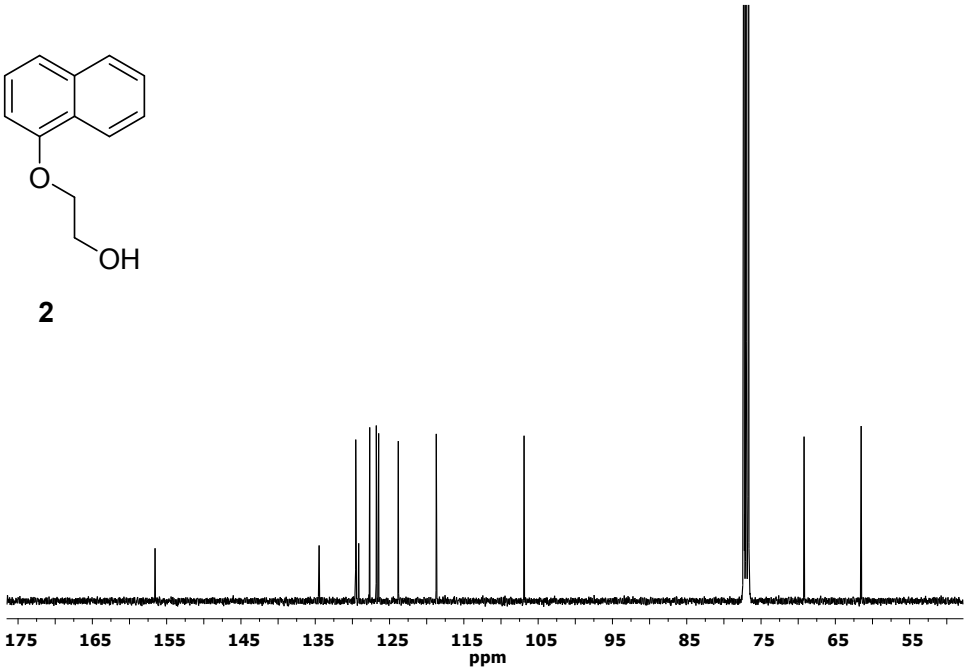

Figure S2. ^{13}C NMR spectrum of **2** in $CDCl_3$.

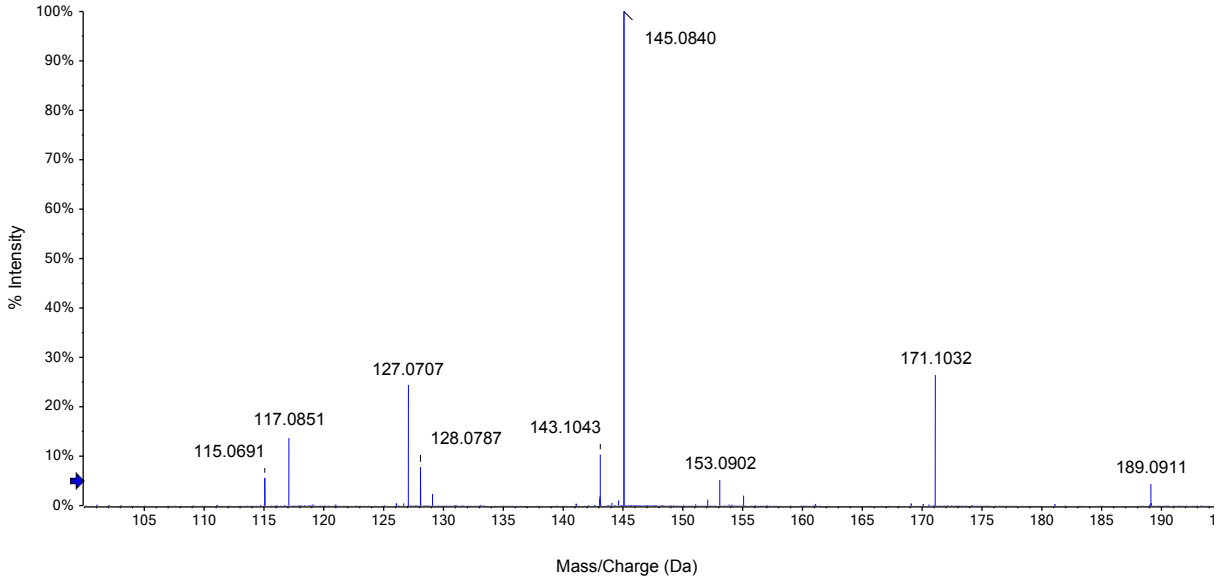

Figure S3. HRMS of compound **2**.

Synthesis of 2-(naphtalen-1yloxy)ethyl 3-(triethoxysilyl)propylcarbamate (3): 2-(1-naphthyloxy)ethanol (**2**, 100 mg, 0.53 mmol) was dissolved in anhydrous ACN (15 mL) and purged with Argon. Then few drops of triethylamine were added to the solution as catalyst. 3-(Triethoxysilyl)propyl isocyanate (132 µl, 0.53mmol) was added dropwise to the solution and the mixture was stirred 48 h at room temperature under Argon atmosphere. Then, the solvent was evaporated under vacuum without any purification (207.59 mg, 0.48 mmol, yield 90%). ^{1}H NMR (400 MHz, CD_3CN) δ: 7.75 (m, 3H), 7.45 (t, J=8.0Hz, 1H), 7.35 (t, J=7.2, Hz 1H), 7.17 (m, 2H), 4.38 (m, 1H), 4.26 (m, 1 H), 4.14 (m, 2H), 3.77 (m, 6H), 3.07 (m, 2H), 1.51 (m, 2H), 1.17 (m, 9H), 0.56 (m, 2H) ppm. ^{13}C NMR (101 MHz, CD_3CN) δ: 157.93, 157.59, 135.70, 130.33, 130.02, 128.52, 127.70, 127.43, 124.63, 119.74, 107.78, 67.68, 63.77, 57.95, 47.00, 24.01, 15.06, 8.01 ppm. HRMS-EI *m/z*: calcd for $C_{22}H_{33}NO_6Si+H^+$: 436.2150; measured: 436.2126.

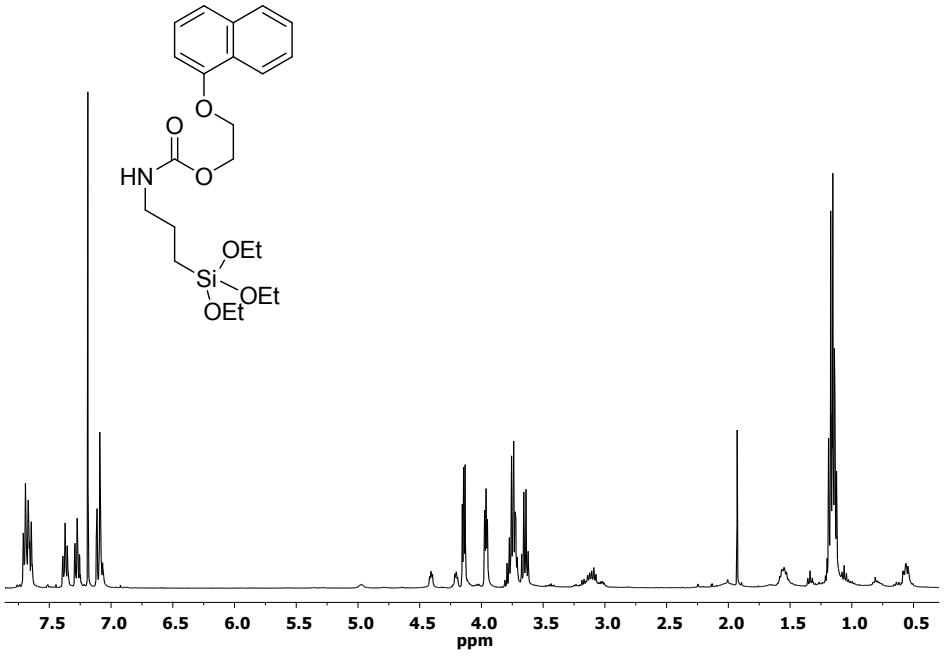

Figure S4. ^{1}H NMR spectrum of **3** in CD_3CN.

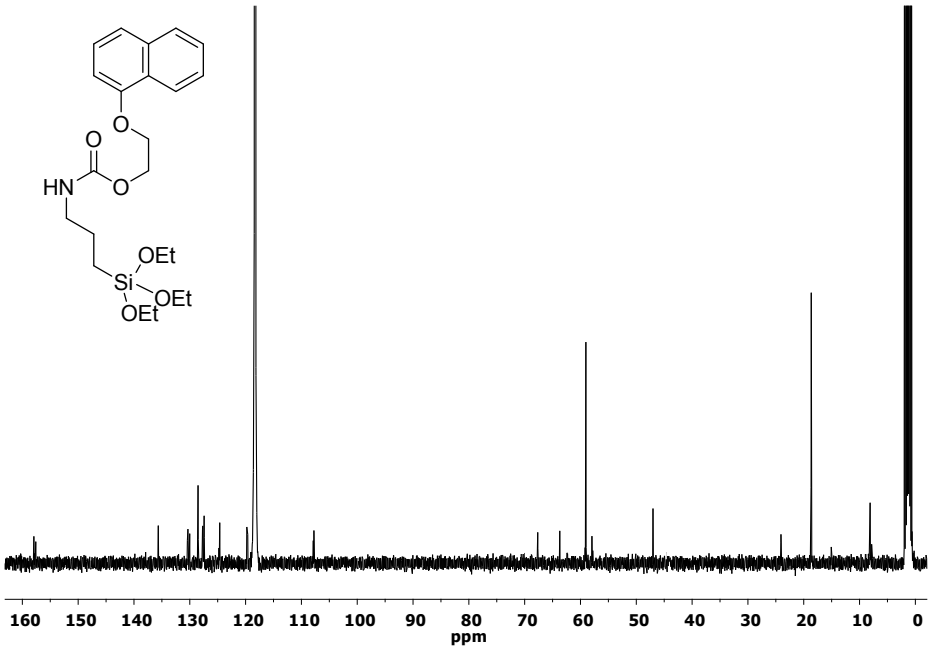

Figure S5. ^{13}C NMR spectrum of **3** in CD_3CN.

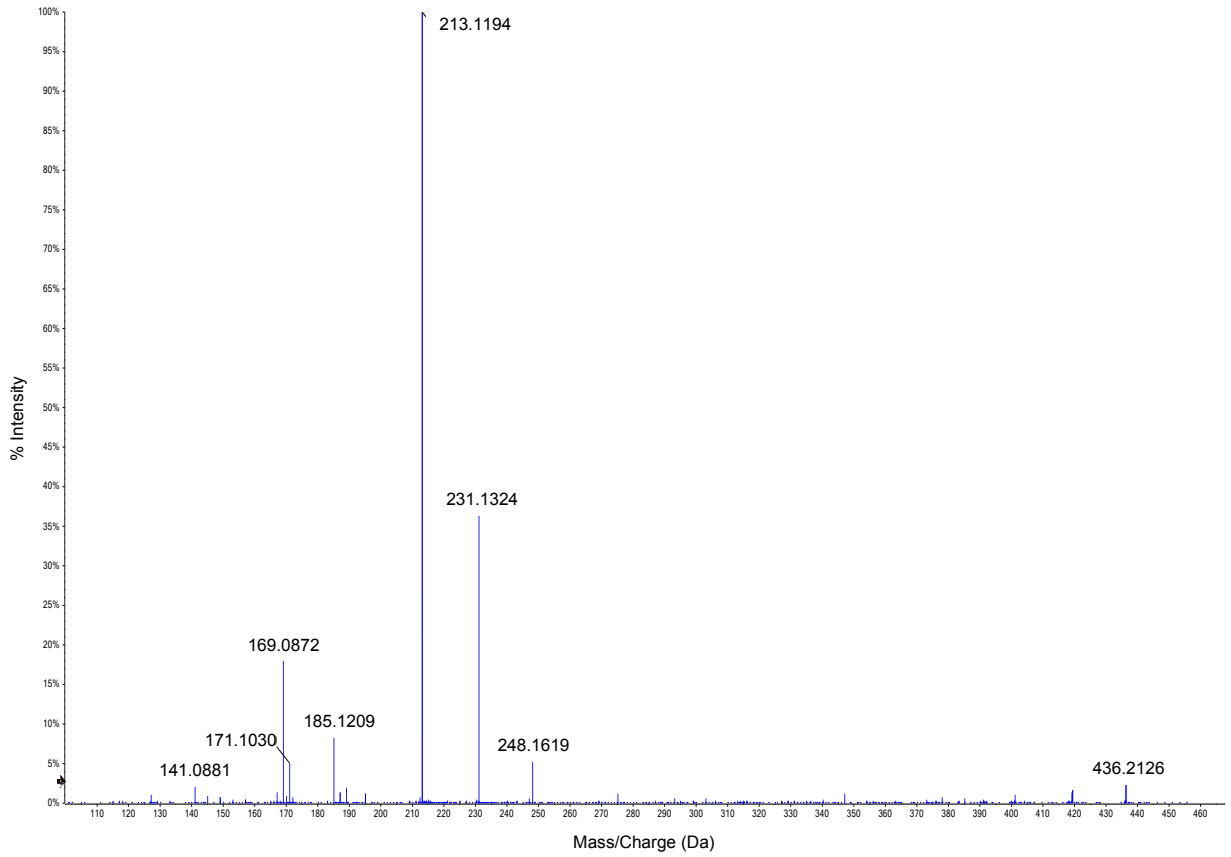

Figure S6. HRMS of compound **3**.

Synthesis of S1: Calcined MCM-41 (200 mg) and fluorescein (53.17 mg, 0.16 mmol) were suspended in CH_3CN (7 mL). The suspension was stirred at room temperature for 24 h in order to load MCM-41 pores. **3** (174.48 mg, 0.4 mmol) was then added, and the final suspension was stirred at room temperature for 5.5 h. The resulting orange solid (**S1**) was isolated by centrifugation, rinsed 3 times with deionized water and with CH_3CN (5 mL), and then dried at 38°C for 18 h.

Synthesis of S2: S1 (15 mg) was suspended in deionized water (3 ml) and $CBPQT^{4+}$ (21 mg, 0.4 mmol) was added. The mixture was stirred for 24 h and then washed 3 times with water to eliminate the residual dye and the uncoordinated $CBPQT^{4+}$.

Characterization of the prepared materials: The MCM-41 scaffold and mesoporous solid **S1** were characterized following standard techniques, including transmission electron microscopy (TEM), powder X-ray diffraction (PXRD) and N_2 adsorption/desorption analysis**.** The PXRD pattern of siliceous MCM-41 nanoparticles as synthesized (Figure 2 in the manuscript, curve a) shows four low-angle reflections

typical of a hexagonal array, indexed as (100), (110), (200) and (210) Bragg peaks. A significant displacement of 3Å of the (100) peak in the PXRD pattern of the MCM-41 calcined nanoparticles is evident in curve b (see Figure 2 in manuscript), related to the further condensation of silanol groups in the calcination step. Finally, curve c (also in Figure 2 in the manuscript) corresponds to the **S1** PXRD pattern. An intensity decrease and a broadening of the (110) and (200) reflections is observed, related to a loss of contrast from filling pore voids with fluorescein dye.

Presence of the mesoporous structure in the final functionalized solids was confirmed by TEM analyses, in which the typical channels of the MCM-41 matrix are visualized as alternate black and white stripes (see Figure 2d and 2e in the manuscript). The figure also shows that the prepared MCM-41 and solid **S1** are obtained as spherical particles with an average diameter of 100 ± 8 nm.

The N_2 adsorption–desorption isotherms of the calcined MCM-41 nanoparticles show an adsorption step at an intermediate P/P_0 value (0.1–0.3), which is typical of this type of solid (see Figure S7, curve a). A total pore volume of 0.54 $cm^3\ g^{-1}$ was calculated by using the BJH model on the adsorption branch of the isotherm. The application of the BET model resulted in a value for the total specific surface of 1260.3 $m^2\ g^{-1}$. A pore diameter of 2.31 nm was determined by porosimetry. The N_2 adsorption–desorption isotherm of **S1** (see Figure S7, curve b) is typical of mesoporous systems with partially filled mesopores. A decrease in the N_2 volume adsorbed (0.36 $cm^3\ g^{-1}$) and surface area (849.0 $m^2\ g^{-1}$) were observed.

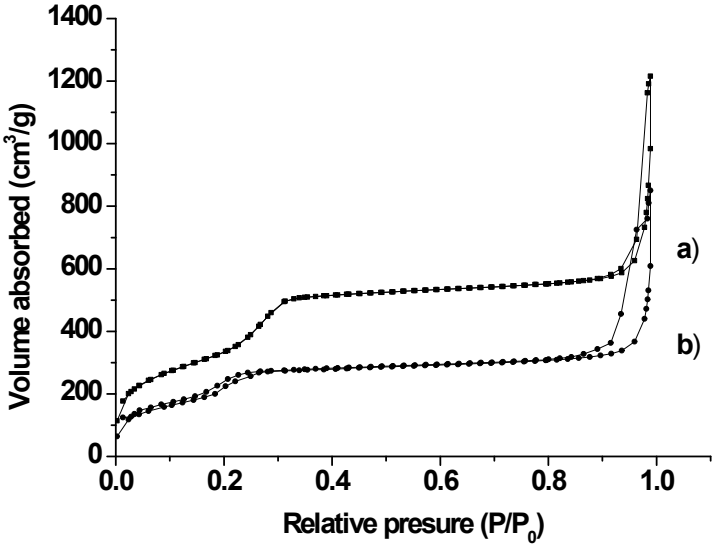

Figure S7. N_2 adsorption-desorption isotherms for (a) calcined MCM-41 nanoparticles and (b) **S1** material.

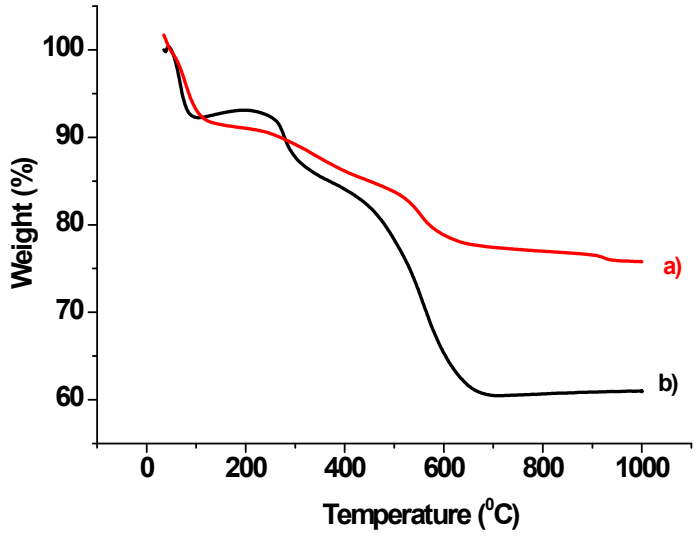

Figure S8. Thermogravimetric analysis for (a) **S1** and (b) **S2** nanoparticles.

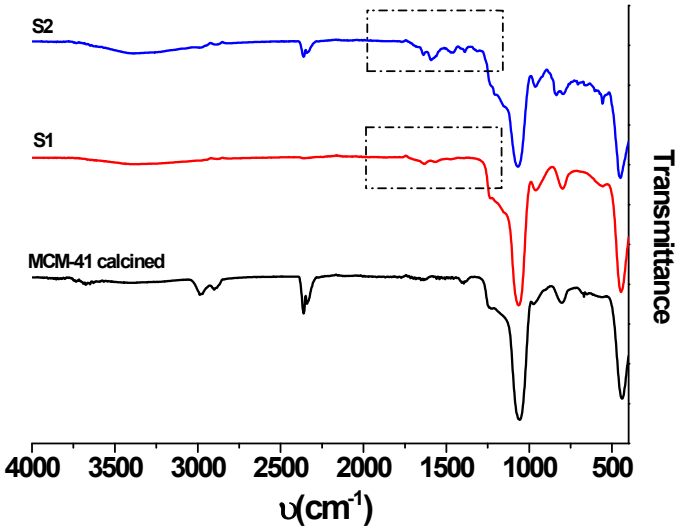

Figure S9. FTIR spectra of calcined MCM-41, **S1** and **S2** nanoparticles.

FTIR spectrum of calcined MCM-41 showed the typical absorption bands at ca. 1100 and 3400 cm^{-1} of the bond stretching vibrations of Si-O-Si and of O-H groups, respectively (see Figure S9). On the other hand, spectra of functionalized **S1** and **S2** nanoparticles showed the bands of the inorganic matrix and C=C stretching vibrations of the aromatic rings (of the grafter naphthalene and coordinated $CBPQT^{4+}$ macrocycle) in the 1400-1600 cm^{-1} range.

Table S1. Elemental analysis for selected materials.

	%C	%H	%N
S1	7.98	2.48	0.27
S2	18.16	3.17	1.35

Elemental analysis of solid **S1** (Table S1) showed the presence of nitrogen (0.27%) that is ascribed to the carbamate moiety of compound **3** grafted in the outer surface of the nanoparticles. The formation of naphthalene⊂$CBPQT^{4+}$ inclusion complexes was assessed also by the elemental analysis of solid **S2** that showed a marked enhancement in nitrogen content (1.35%). This enhancement could be clearly ascribed to the $CBPQT^{4+}$ that covered the outer surface of **S2**. From

thermogravimetric and elemental analysis studies, contents of 0.87 and 0.80 mmol g^{-1} of solid for fluorescein and **3** (in **S1**) and 0.83, 0.73 and 0.23 mmol g^{-1} of solid for fluorescein, **3** and $CBPQT^{4+}$ (in **S2**) were calculated.

Release experiments of solid S2 in the presence of MDMA: To investigate the gating properties of **S2**, 1mg of this solid was suspended in 400 μL of deionized water and separated in two aliquots of 200 μL. Both samples were filled to a volume of 1200 μL with water. At the same time, 100 μL of MDMA (100 mM) were added to one aliquot. Simultaneously, 100 μL of water were added to the remaining aliquot. Both suspensions were stirred at 25ºC for 120 min. Aliquots of 150 μL were taken at several times and centrifuged for 2 min at 12000 rpm (to remove the solid) and the fluorescence of the released fluorescein was measured at 520 nm (λ_{exc} = 495 nm). The release profile of **S2** in presence and in absence of MDMA is shown in the manuscript (Figure 2).

Calibration curve of S2 with MDMA: In order to carry out these experiments, 1 mg of **S2** was suspended in 1120 μL of deionized water and divided into 11 aliquots of 100 μL each. Several water solutions of MDMA that fell within a range from 10^{-8} to 10^{-3} M were prepared and, instantaneously, 200 μL of each MDMA solutions were added to the aliquots and stirred for 10 min. One aliquot was reserved to add 200 μL of water as a blank. Then suspensions were centrifuged for 2 min at 12000 rpm (to remove the solid) and the fluorescence of the released fluorescein was measured at 520 nm (λ_{exc} = 495 nm). From the calibration curve showed in Figure S10 a limit of detection of 4.9 μM for MDMA was measured.

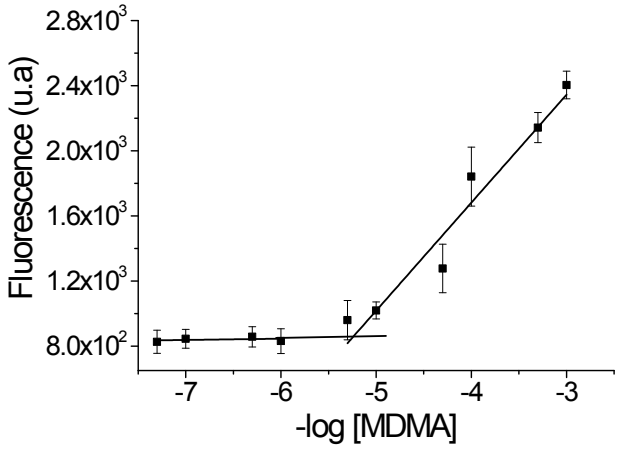

Figure S10. Release of fluorescein from solid **S2** in the presence of different amounts of MDMA in water at pH 7.0 after 10 min of addition. Error bars are expressed as 3σ for three independent experiments.

Selectivity studies with S2: In order to test the selectivity of **S2**, 3.5 mg of the solid were suspended in 1.4 mL water and divided into 7 aliquots of 100 μL. Several water solutions of different drugs (MDMA, morphine, methadone, heroin and cocaine), at a concentration of 100 mM were prepared. Next 100 μL of the prepared solutions were added to each **S2** aliquot to obtain a final concentration of 1 mM. One aliquot was reserved to add 100 μL of water as a blank. Finally, each aliquot was filled to 1500 μL. After 10 min of stirring, samples were centrifuged for 2 min at 12000 rpm (to remove the solid) and the fluorescence of the released fluorescein was measured at 520 nm (λ_{exc} = 495 nm), (see Figure 4 in the manuscript).

Release experiments of solid S1 in the presence of MDMA: 1 mg of this solid was suspended in 400 μL of deionized water and separated in two aliquots of 200 μL. Both samples were filled to a volume of 1200 μL with water. At the same time, 100 μL of MDMA (100 mM) were added to one aliquot. Simultaneously, 100 μL of water were added to the remaining aliquot. Both suspensions were stirred at 25ºC for 120 min. Aliquots of 150 μL were taken at several times and centrifuged for 2 min at 12000 rpm (to remove the solid) and the fluorescence of the released fluorescein was measured at 520 nm (λ_{exc} = 495 nm). The release profiles of **S1** in absence and in presence of MDMA are shown in Figure S11.

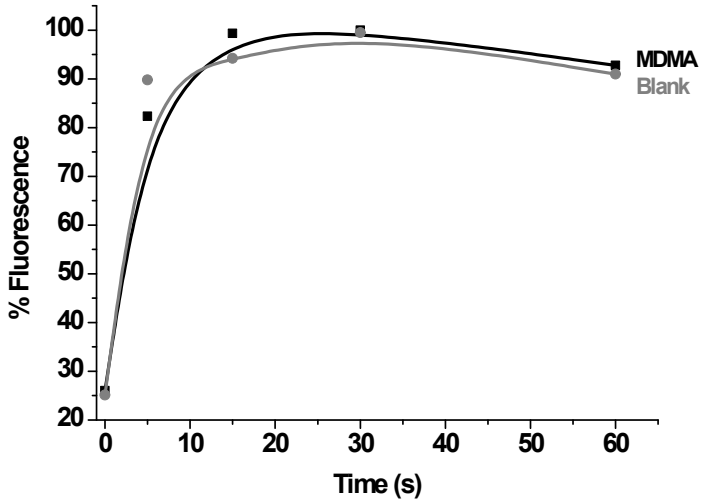

Figure S11. Release profiles of fluorescein from aqueous suspensions of solid **S1** at pH 7.0 in the absence and in the presence of MDMA (10 μmol).

As could be seen in the release profiles obtained for solid **S1** in the absence and in the presence of MDMA a marked fluorescein release was observed in both cases. These facts pointed out the important role played by the pseudorotaxane-based supramolecular structure in the controlled release features of solid **S2**.

Stability constant calculation: The shifts of the ^{1}H NMR signals of $CBPQT^{4+}$ upon addition of increasing quantities of MDMA in D_2O were used to calculate the stability constant for the inclusion complex. The obtained profile is shown in Figure S12. The data fitted well to a 1:1 MDMA-$CBPQT^{4+}$ stoichiometry inclusion complex and the calculated stability constant amounted to log K = 2.65 ± 0.25. The measured value is roughly similar to that described by Kaifer and co-workers (*J. Am. Chem. Soc.* 1992, **114**, 10624) for the closely related dopamine molecule (log K = 3.03) which also formed 1:1 inclusion complex with $CBPQT^{4+}$ in a highly competitive media such as PBS.

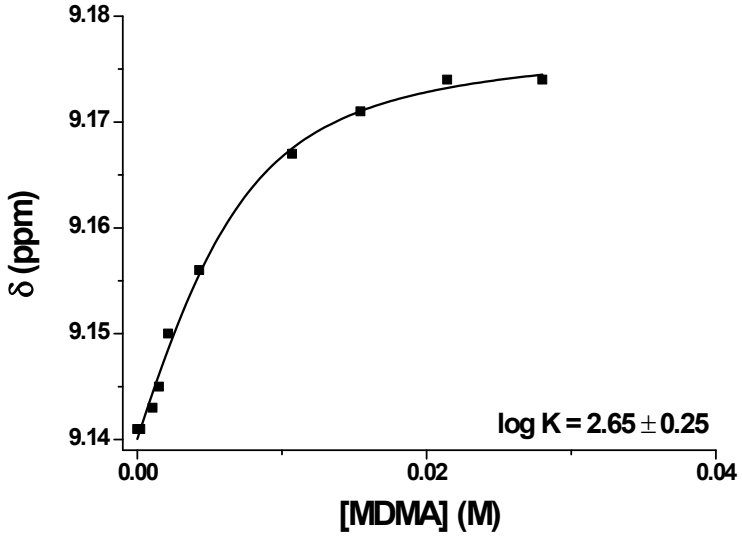

Figure S12. ^{1}H NMR titration profile of $CBPQT^{4+}$ upon addition of increasing MDMA quantities in D_2O. The fitting of the experimental data to a 1:1 stoichiometry inclusion complex is also shown.

MDMA detection in real samples: MDMA is usually consumed integrated in ecstasy tablets and not in its pure form. Normally, different adulterants or excipients are added to reduce the final price. To test the possible application of **S2** material for detecting MDMA in real samples, we prepared a simulated tablet and studied the detection of this drug within a real possible interfering matrix. The composition of the tablets may widely vary. We have used to prepare ecstasy tablets 45% of MDMA, 18.3% of sucrose, 18.3% of chalk and 18.3% of paracetamol. For this purpose, 1 mg of **S2** was suspended in 620 μL of distilled water and divided in 6 aliquots of 100 μL. Moreover we prepared:

- 100 μl solution of MDMA (45%)

-100 μl solution of a filtered chalk dispersion (18.3%)

-100 μl solution of sucrose (18.3%)

-100 μl solution of paracetamol (18.3%)

-100 μl solution of ecstasy (MDMA (45%) + chalk (18.3%) + sucrose (18.3%) + paracetamol (18.3%))

For the blank, 200 μl of water were added to 100 μl of **S2** suspension. For the samples, 100 μl of water were added to 100 μl of **S2** suspension and, additionally, 100 μl of each prepared solution or a mixture of

all of them (to simulate an ecstasy tablet). After 10 min of stirring, samples were centrifuged for 2 min at 12000 rpm (to remove the solid) and the fluorescence of the released fluorescein was measured at 520 nm (λ_{exc} = 495 nm). The obtained results are shown in Figure S13.

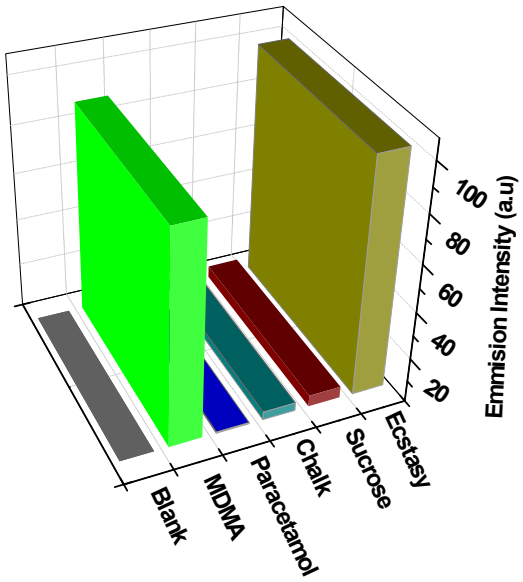

Figure S13. Emission intensity of fluorescein at 520 nm (excitation at 495 nm) released from **S2** nanoparticles (water pH 7.0) in the presence of components of an ecstasy tablet.

As could be seen in Figure S13, only MDMA (alone or mixed with the other ecstasy tablet components) is able to induce pseudorotaxane dethreading with subsequent pore opening and fluorescein release.